

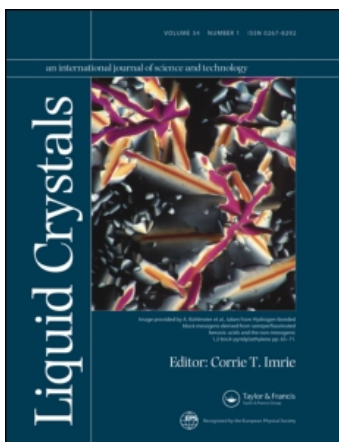
This article was downloaded by: [TIB-Lizenzen - TIB Licence Affairs]

On: 12 December 2008

Access details: Access Details: [subscription number 777306419]

Publisher Taylor & Francis

Informa Ltd Registered in England and Wales Registered Number: 1072954 Registered office: Mortimer House, 37-41 Mortimer Street, London W1T 3JH, UK



## Liquid Crystals

Publication details, including instructions for authors and subscription information:

<http://www.informaworld.com/smpp/title-content=t713926090>

### Molecular ordering in microconfined liquid crystals: An infrared linear dichroism study

H. Binder <sup>a</sup>; H. Schmiedel <sup>a</sup>; G. Lantzsch <sup>a</sup>; C. Cramer <sup>a</sup>; G. Klose <sup>a</sup>

<sup>a</sup> Fakultät für Physik, Geowissenschaften der Universität Leipzig, Leipzig, Germany

Online Publication Date: 01 September 1996

**To cite this Article** Binder, H., Schmiedel, H., Lantzsch, G., Cramer, C. and Klose, G. (1996) 'Molecular ordering in microconfined liquid crystals: An infrared linear dichroism study', *Liquid Crystals*, 21:3, 415 — 426

**To link to this Article:** DOI: 10.1080/02678299608032850

**URL:** <http://dx.doi.org/10.1080/02678299608032850>

PLEASE SCROLL DOWN FOR ARTICLE

Full terms and conditions of use: <http://www.informaworld.com/terms-and-conditions-of-access.pdf>

This article may be used for research, teaching and private study purposes. Any substantial or systematic reproduction, re-distribution, re-selling, loan or sub-licensing, systematic supply or distribution in any form to anyone is expressly forbidden.

The publisher does not give any warranty express or implied or make any representation that the contents will be complete or accurate or up to date. The accuracy of any instructions, formulae and drug doses should be independently verified with primary sources. The publisher shall not be liable for any loss, actions, claims, proceedings, demand or costs or damages whatsoever or howsoever caused arising directly or indirectly in connection with or arising out of the use of this material.

# Molecular ordering in microconfined liquid crystals: An infrared linear dichroism study

by H. BINDER\*, H. SCHMIEDEL, G. LANTZSCH, C. CRAMER and  
G. KLOSE

Fakultät für Physik und Geowissenschaften der Universität Leipzig, Linnèstr. 5,  
D-4103 Leipzig, Germany

(Received 15 March 1996; accepted 12 April 1996)

The molecular arrangement of 5CB confined within the cylindrical pores of Anopore membranes was characterized by means of the IR-order parameter obtained from linear dichroism measurements of selected IR absorption bands. The treatment of the experimental data includes a local field correction extended to the twisted nematic configuration, yielding order parameters increased by about 30% in comparison with the uncorrected data. The nematic director of 5CB aligns along the pore axes, whereas in lecithin coated Anopore channels, the local nematic director is oriented approximately radially due to the perpendicular anchoring of the 5CB molecules at the pore wall. Doping of 5CB with the chiral agent CB15 yields local nematic directors tilted with respect to the pore axes. The average tilt angle increases up to about 40° at a fraction of CB15,  $x_{CB15} = 0.25$  (w/w). These results are discussed in terms of the conical helicoidal and alternatively the radially twisted axial arrangement of the LC molecules within submicrometer cylindrical cavities.

## 1. Introduction

The interactions between liquid crystals (LC) and amorphous surfaces determine, in combination with the liquid crystal elastic energy (Frank's elastic energy), the director field in microconfined liquid crystalline droplets [1] and cylinders [2]. Crawford *et al.* [2, 3] and Vrbancic *et al.* [4] studied the molecular order and dynamics in the isotropic and nematic phases of nematic substances adsorbed in the cylindrical channels of inorganic Anopore membranes (AP) [5]. They provide an ideal system for the investigation of surface interactions and anchoring properties at solid-liquid interfaces, because of their high inner surface to volume ratio. Dependent on the surface anchoring, three basic types of nematic director field configuration are reported: uniform axial for parallel axial (planar) anchoring, planar polar for homeotropic anchoring [6] and planar bipolar for parallel tangential anchoring [7]. The surface anchoring conditions can be modified by several coupling agents such as surfactants or polymers [3, 6].

Chiral nematic liquid crystals (cholesteric or twisted nematic) filled into submicrometer cavities have been investigated by several authors in order to relate the effect of a curved confining geometry to the chiral structures formed under homeotropic as well as planar anchoring conditions [8-12]. However, both planar and

homeotropic orientation at the walls, as observed in the nematic systems, are incompatible with an undisturbed helicoidal director field inside the channels. Hence, a number of possible structures with bulk and surface disclination lines have been predicted and observed in cylindrical capillaries [9, 10]. Furthermore, different possible director configurations of chiral liquid crystals in cylindrical cavities have been derived theoretically depending on the anchoring conditions [13].

On the basis of  $^2\text{H}$  NMR measurements, two twisted nematic director field configurations in the cylindrical pores of untreated Anopore membranes with planar anchoring of the LC molecules are proposed: the radially twisted axial (RTA) configuration and the axially twisted bipolar (ATPB) configuration [14]. A transition from an RTA to an ATPB structure was induced with decreasing pitch length. Alternatively, the results of optical,  $^1\text{H}$  NMR and  $^{13}\text{C}$  NMR investigations on similar systems are interpreted in terms of a conical helicoidal (CH) director field [11, 12]. The ATPB and CH configurations twist along the cylinder axis, whereas the twist of the RTA configuration is along the radial direction.

In general the molecular arrangement within micropores filled with chiral LC remains in many details an open question up to now. Several techniques are used in order to extract information about the molecular order in microconfined LC materials, permitting unfortunately no unequivocal decision between different alternative structural models. Optical methods such as the

\* Author for correspondence.

measurement of the optical activity and birefringence yield important information about the chirality and symmetry of molecular packing within the sample, but mainly only in a more qualitative sense [11, 15].  $^2\text{H}$  NMR provides a direct measure of the orientational order at the molecular level via the time averaged quadrupolar-splitting frequency from a selectively deuterated LC molecule and has been used to investigate different microconfined LC structures [2, 3, 6, 7, 14, 16], including nematic [6] and chiral nematic [11, 14] liquid crystals in Anopore membranes. Further insight into the orientational order may be obtained from the chemical shift in  $^{13}\text{C}$  NMR spectroscopy, yielding the director distribution density with respect to the Anopore channel axes [11, 12]. However molecular diffusion within the NMR time scale distorts the spectra. Hence an adequate analysis needs to obtain additional information about the molecular dynamics in the system investigated.

Infrared absorption dichroism spectroscopy, on the other hand, represents a reasonably simple and well established technique to measure the molecular order parameter in uniaxial liquid crystals [17–20, 25] and hence its application to microconfined LC samples appears to be relevant.

We report an IR dichroism study on the molecular arrangement of LC in Anopore membranes. A correction factor for local field effects on the measured dichroic ratios was derived on the basis of the ellipsoidal cavity model [17, 19]. The temperature dependence of the molecular order parameter,  $S_{\text{mol}}$ , of 5CB in untreated and lecithin coated Anopore, i.e. with planar and homeotropic anchoring, respectively, was obtained and compared with corresponding bulk data. The average tilt angle of the local director with respect to the pore axes was determined for twisted nematic liquid crystals at different pitch lengths of the respective bulk systems. The results are discussed in relation to different models of chiral phases in submicroscopic cylinders.

## 2. Materials and methods

### 2.1. Substances and sample preparation

The liquid crystal material was 4-cyano-4'-pentylbiphenyl (5CB) and the chiral dopant 4-cyano-4'-(2-methylbutyl)biphenyl (CB15). Pieces of Anopore membranes (length 20 mm, width 10 mm, thickness  $60\ \mu\text{m}$  and pore diameter  $0.2\ \mu\text{m}$ ) were filled with 5CB and/or 5CB/CB15 mixtures at a temperature above the nematic–isotropic phase transition temperature. The samples were carefully cleaned to remove additional LC material from the outer surfaces of the membranes. Homogeneity of the samples was proved by optical polarizing microscopy. The inner surface of the Anopore was treated with the lecithin (1,2-dimyristoyl-*sn*-glycero-3-phosphotidylcholine) by capillary-filling an

ethanolic solution of the lecithin (50 mM) into the membrane and then placing the sample into a vacuum chamber for several hours in order to remove the solvent.

### 2.2. Infrared measurements

Infrared spectra were recorded on a BioRad FTS-60a Fourier transform infrared spectrometer equipped with a deuterated triglycine sulphate (DTGS) detector. 256 interferograms, collected with an optical velocity of  $1.58\ \text{mm s}^{-1}$  and a maximum optical retardation of 5.4 mm, were co-added, apodized with a triangular function, and Fourier transformed with one level of zero filling to yield a spectral resolution of  $2\ \text{cm}^{-1}$  and data encoded every  $1\ \text{cm}^{-1}$ .

Anopore membranes of about  $10 \times 20\ \text{mm}^2$  size were placed between  $\text{CaF}_2$  windows ( $15 \times 30\ \text{mm}^2$ ) and mounted into a home built goniometer cell thermostated by flowing water. Temperatures were controlled by a Pt-100 thermocouple placed against the edge of the cell window. FTIR spectra were recorded as a function of temperature in steps of one degree, allowing the sample to equilibrate for at least 10 min after reaching the prescribed temperature in each step. No systematic differences between heating and cooling scans were observed.

In the standard configuration, the angle of incidence of the IR beam was  $\omega = 45^\circ$  with respect to the membrane normal (cf. figure 1). In some cases  $\omega$  was varied from  $0^\circ$  to  $60^\circ$  in steps of  $5^\circ$ . A wire grid polarizer with an efficiency of  $>98\%$  was placed behind the sample cell. Each spectrum was measured at two perpendicular

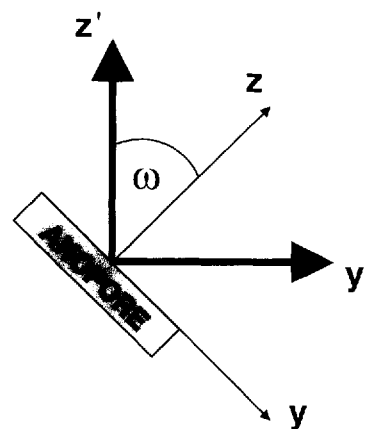


Figure 1. Definition of axis systems:  $\{x', y', z'\}$  laboratory frame;  $\{x, y, z\}$  director frame;  $\omega$  is the angle of incidence. The IR beam propagates along  $z'$  and is polarized with the polarizer aligned along  $x'$  and  $y'$  to yield the absorbances  $A_{\perp}$  and  $A_{\parallel}$  after passing the Anopore sample. The optical axis of the sample is parallel to  $z$ . The parallel  $x$ - and  $x'$ -axes being oriented perpendicularly to the  $yz$ -plane are omitted for clarity.

polarizations of the IR beam adjusted by aligning the polarizer to the vertical and horizontal directions, i.e. parallel to the  $x$  and  $y$  axes of the laboratory frame (see below).

Absorbance spectra of LC in Anopore membranes were calculated using the respective single channel spectrum of an empty Anopore membrane (without LC) as background. The dichroic ratios of selected absorption bands were calculated using integrated absorbances.

### 2.3. Refractometry

Indices of refraction of 5CB for wavelengths of 480, 509, 644 nm (Na-lamp) and 435, 546, 578 nm (Hg-lamp) were measured using wedge-shaped LC cells (wedge angle  $27^\circ$ ) under conditions for minimum ray deviation in a prism. The orientation of the LC director along the cross-section line of the faces of the prism was achieved by a magnetic field ( $B \approx 0.8$  T). The ray deviation angle was measured by means of a precision goniometer spectrometer. Temperature stabilization was better than 0.1 K and the precision of the measured indices of refraction was about  $+1 \times 10^{-4}$ .

## 3. IR dichroism and the molecular order of liquid crystals

### 3.1. Bulk nematics

Referring to figure 1, we define a cartesian system  $\{x, y, z\}$  with  $z$  parallel to the optical axis of the sample given by the director of the nematic liquid crystal, and a laboratory frame  $\{x', y', z'\}$  in which the polarization direction of the IR beam is defined. The  $z$ -axis includes the angle of incidence,  $\omega$ , with  $z'$ , the propagation direction of the light outside of the sample. Consequently, the rotation from the  $\{x, y, z\}$ -frame to  $\{x', y', z'\}$  is completely specified by the angle  $\omega$ .

Suppose the incident electromagnetic wave is polarized parallel to  $x'$  (vertical orientation of the polarizer) or  $y'$  (horizontal orientation) then the corrected absorbances of an infrared band caused by a macroscopic ensemble of absorbing molecules are given by [17, 19–22]

$$\begin{aligned} A_{x'} &= A_{\perp} \propto \frac{f_{\perp}^2}{n_{\perp}} \langle \mu_x^2 \rangle \\ A_{y'} &= A_{\omega} \propto \frac{f_{\perp}^2}{n_{\perp}} \langle \mu_y^2 \rangle \cos^2 \omega' + \frac{f_{\parallel}^2}{n_{\parallel}} \langle \mu_z^2 \rangle \sin^2 \omega' \end{aligned} \quad (1)$$

On account of the uniaxial symmetry of the system with respect to the  $z$ -axis the substitutions  $\parallel \equiv z$  and  $\perp \equiv x = y$  are used for the indices. Consequently,  $n_{\parallel}$  and  $n_{\perp}$  are the refractive indices and  $f_{\parallel}$  and  $f_{\perp}$  the local field factors for light polarizations parallel and perpendicular to the nematic director [19, 23, 24].

The angle between the optical axis and the propaga-

tion direction of the horizontal polarized IR beam within the sample,  $\omega'$ , is related to the angle of incidence,  $\omega$ , through Snell's law according to

$$\sin \omega' = \frac{\sin \omega}{\bar{n}} \quad (2)$$

with

$$\bar{n} = n_{\perp} [1 - \sin^2 \omega (n_{\parallel}^{-2} - n_{\perp}^{-2})]^{1/2}. \quad (3)$$

The ensemble averaging of the squared projections of the IR active transition dipole moment onto the  $x$ -,  $y$ - and  $z$ -axes denoted in equation (1) by the angular brackets yields within the system of uniaxial symmetry:

$$\begin{aligned} \langle \mu_x^2 \rangle &= \langle \mu_y^2 \rangle \propto (1 - S_{\text{opt}}) \\ \langle \mu_z^2 \rangle &\propto (1 + 2S_{\text{opt}}) \end{aligned} \quad (4)$$

with the optical order parameter

$$S_{\text{opt}} = S_{\text{mol}} S_{\text{bond}}. \quad (5)$$

The macroscopic orientational order of the long principal axis of the molecule is characterized by the molecular order parameter

$$S_{\text{mol}} = \frac{1}{2}(3 \langle \cos^2 \theta_{\text{mol}} \rangle - 1) \quad (6)$$

where  $\theta_{\text{mol}}$  is the angle between the director of the system and the long principal axis of a selected molecule. Analogously, the bond order parameter,  $S_{\text{bond}}$ , is given as a function of  $\theta_{\text{bond}}$  which specifies the angle between the transition dipole moment and the long principal axis of the molecule. In this case the mean value  $\langle \cos^2 \theta_{\text{bond}} \rangle$  considers the fact that, on the one hand, the molecule possibly contains more than one identical atomic group with transition dipole moments having, however, different orientations with respect to the molecular axis. On the other hand the orientation of the transition dipole may be characterized by a variable angle  $\theta_{\text{bond}}$ ; for example if the respective atomic group belongs to a flexible part of the molecule. Hence,  $S_{\text{bond}}$  is the average bond order parameter considering all orientations of the respective transition dipole with respect to the molecular axis.

Finally, using equation (1) together with equations (2) and (4), the dichroic ratio of the infrared band, defined as  $R = A_{y'}/A_{x'}$ , can be related to the optical order parameter according to the following equation:

$$R = 1 + \frac{\sin^2 \omega S_{\text{opt}}(2g^{-1} + 1) + (g^{-1} - 1)}{\bar{n}^2 (1 - S_{\text{opt}})} \quad (7)$$

with the correction factor

$$g = \frac{n_{\parallel}}{n_{\perp}} \left( \frac{f_{\perp}}{f_{\parallel}} \right)^2 \quad (8)$$

depending on the refractive indices of the ordinary and

extraordinary IR beam and the local field factors. The  $g$ -factor takes into account the anisotropic optical properties of the nematic LC modifying the electric field vector of light locally, and thus the absorbance of the sample [19, 20, 24].

### 3.2. Determination of the correction factor

#### 3.2.1. Refractive indices and molecular order parameter in bulk nematics

Refractive indices,  $n_{\parallel}$  and  $n_{\perp}$ , of bulk 5CB were measured at selected wavelengths in the range 435–644 nm as a function of the temperature (cf. figure 2). Fitting of the data to the empirical dispersion equation

$$n_{\parallel,\perp}(\lambda) = \left[ 1 + \frac{A_{\parallel,\perp}(T)\lambda^2}{\lambda^2 - B_{\parallel,\perp}(T)} \right]^{1/2} \quad (9)$$

at selected temperatures yields the coefficients  $A_{\parallel,\perp}(T)$  and  $B_{\parallel,\perp}(T)$ . In accordance with [17, 19], we found  $B_{\parallel,\perp}(T) < 0.04 \mu\text{m}^2$  and therefore in the mid IR region, i.e. for wavelengths  $\lambda > 3 \mu\text{m}$ , the refractive indices are calculated to a good approximation by

$$n_{\parallel,\perp} \cong [1 + A_{\parallel,\perp}(T)]^{1/2}. \quad (10)$$

IR order parameters of oriented samples of 5CB are reported by several authors [17–19]. Using the temperature dependence of the corrected optical order parameter of the CN-stretching band obtained in reference [19],  $S_{\text{opt}}(\text{CN}) = (1 - T/T_{\text{NI}})^{0.16}$ , we correlated  $S_{\text{opt}}(\text{CN})$  with the refractive indices determined (cf. figure 3). Obviously a linear correlation between both quantities

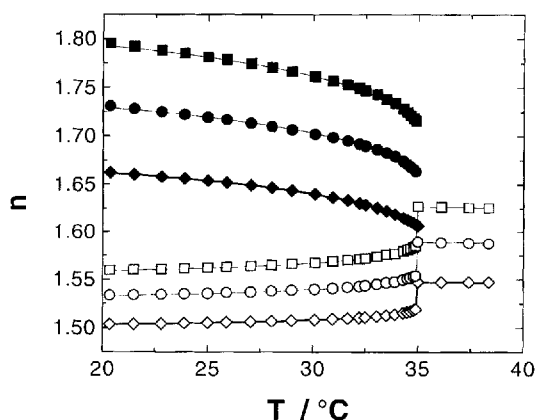


Figure 2. Refractive indices,  $n_{\parallel}$  (solid symbols) and  $n_{\perp}$  (open symbols), of bulk 5CB as a function of temperature measured at wavelengths  $\lambda = 435 \text{ nm}$  ( $\blacksquare$ ,  $\square$ ) and  $578 \text{ nm}$  ( $\bullet$ ,  $\circ$ ). The respective refractive indices in the IR spectral region are calculated by means of equation (10) with  $\lambda = 5000 \text{ nm}$  ( $\blacklozenge$ ,  $\diamond$ ).  $n_{\parallel}$ - and  $n_{\perp}$ -data measured at 480, 509, 546, 578 and 644 nm are not shown.

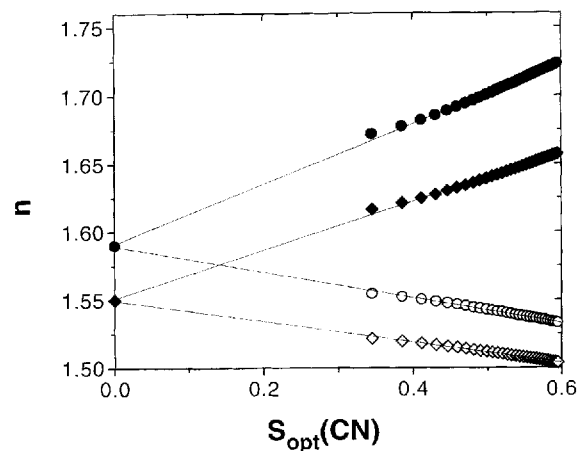


Figure 3. Correlation between the CN-order parameter,  $S_{\text{opt}}(\text{CN})$ , and the refractive indices  $n_{\parallel}$  and  $n_{\perp}$  in the VIS-range at  $\lambda = 578 \text{ nm}$  ( $\bullet$ ,  $\circ$ ) and in the IR ( $\tilde{\nu} = 2000 \text{ cm}^{-1}$ ) ( $\blacklozenge$ ,  $\diamond$ ). The lines represent linear fits according to equation (11) with  $K_{\parallel} = 0.220$ ,  $K_{\perp} = -0.094$ ,  $n_{\text{iso}} = 1.59$  (578 nm) and  $K_{\parallel} = 0.178$ ,  $K_{\perp} = -0.076$ ,  $n_{\text{iso}} = 1.55$  ( $2000 \text{ cm}^{-1}$ ). The regression coefficients of the fits are better than 0.9989.

can be established empirically, i.e.

$$n_{\parallel,\perp} \cong n_{\text{iso}} + K_{\parallel,\perp}(\lambda)S_{\text{opt}}(\text{CN}). \quad (11)$$

$n_{\text{iso}}$  denotes the refractive index of the isotropic sample. From the linear dependence given by equation (11) it follows directly that the birefringence should also be proportional to the order parameter, i.e.

$$\Delta n = n_{\parallel} - n_{\perp} \cong [K_{\parallel}(\lambda) - K_{\perp}(\lambda)]S_{\text{opt}}(\text{CN}). \quad (12)$$

As expected, a linear correlation between  $\Delta n$  and  $S_{\text{opt}}(\text{CN})$  is also evident from the results given in reference [19] where an identical temperature dependence of the birefringence at 644 nm and the IR order parameter (namely  $S_{\text{opt}}(\text{CN})$ ,  $\Delta n \sim (1 - T/T_{\text{NI}})^{0.16}$ ) was obtained. In general the interrelation between the  $\Delta n$  and the order parameter derived by several authors is more complicated [20, 24]. However, in the present case the deviation from linearity is small and therefore the linear approximation given above seems to be sufficiently accurate to calculate the correction factor for the IR dichroic ratio given by equation (7).

#### 3.2.2. Local field correction

Within a uniaxially ordered system the local field factors appearing in equations (1) and (8) are usually expressed in terms of the diagonal components of the Lorentz factor tensor,  $L_{\parallel}$  and  $L_{\perp}$ , according to [17, 19, 23]

$$f_{\parallel,\perp} = 1 + L_{\parallel,\perp}(n_{\parallel,\perp}^2 - 1). \quad (13)$$

The Lorentz factor can be calculated within the frame

of the ellipsoidal cavity model [17, 19], where  $L_{\parallel}$  and  $L_{\perp}$  are related to the normalized birefringence,  $\Delta n/\Delta n_{\max}$ .  $\Delta n_{\max}$  denotes the maximum birefringence corresponding to perfect molecular order, i.e.  $S_{\text{mol}} = 1$ . Assuming  $S_{\text{mol}} = S_{\text{opt}}(\text{CN})$  (see below) and making use of the linear correlation between  $\Delta n$  and  $S_{\text{opt}}(\text{CN})$  established in equation (12), the normalized birefringence is just the order parameter, i.e.  $\Delta n/\Delta n_{\max} \cong S_{\text{mol}}$ . Consequently, the diagonal components of the Lorentz factor can be written as a function of the molecular order parameter

$$\begin{aligned} L_{\perp} &= \frac{1}{3} + (L_{\perp, \max} - \frac{1}{3})S_{\text{mol}} \\ L_{\parallel} &= \frac{1}{3} - 2(L_{\perp, \max} - \frac{1}{3})S_{\text{mol}}. \end{aligned} \quad (14)$$

$L_{\perp, \max}$ , the maximum value of  $L_{\perp}$ , was evaluated for a cavity of ellipsoidal shape formed by a 5CB molecule in the surrounding matrix, assuming a ratio of the semi-axes of 3·4 [26] or 4–5 [19] to yield  $L_{\perp, \max} = 0.452$  and 0.462–0.472, respectively.

After combining equations (8), (13) and (14), the correction factor is expressed as a function of the molecular order parameter

$$g(S_{\text{mol}}) = \frac{n_{\parallel}}{n_{\perp}} \left\{ \frac{1 + [\frac{1}{3} + (L_{\perp, \max} - \frac{1}{3})S_{\text{mol}}](n_{\perp}^2 - 1)}{1 + [\frac{1}{3} - 2(L_{\perp, \max} - \frac{1}{3})S_{\text{mol}}](n_{\parallel}^2 - 1)} \right\}^2 \quad (15)$$

where the refractive indices also represent functions of  $S_{\text{mol}}$  approximated by the linear correlation given in equation (11).

Finally, rearrangement of equation (7) and substitution of equation (5) yields the molecular order parameter as a function of the dichroic ratio determined experimentally

$$S_{\text{mol}} = S_{\text{bond}}^{-1} \frac{R - A(S_{\text{mol}})}{R + B(S_{\text{mol}})} \quad (16)$$

with

$$\begin{aligned} A(S_{\text{mol}}) &= \frac{\sin^2 \omega}{\bar{n}^2} [g(S_{\text{mol}})^{-1} - 1] + 1 \\ B(S_{\text{mol}}) &= \frac{\sin^2 \omega}{\bar{n}^2} [2g(S_{\text{mol}})^{-1} + 1] - 1. \end{aligned} \quad (17)$$

### 3.3. Tilted nematics in cylindrical pores

We assume a twisted nematic ( $N^*$ ) phase confined to a cylindrical cavity where the local nematic director is tilted axially symmetric with respect to the pore axis by a constant tilt angle,  $\theta_{\text{tilt}}$ . The local field correction given in §3.1 assumes uniform nematic ordering. Consequently the treatment of IR dichroism data in  $N^*$  phases has to take into consideration the tilt of the local director relative to the symmetry axis within the frame of the ellipsoidal cavity model [17]. In this case the refractive indices of light polarized perpendicular and parallel to

the pore axis represent averaged values of  $n_{\parallel}$  and  $n_{\perp}$ , corresponding to untilted, i.e. nematic LC ( $\theta_{\text{tilt}} = 0^\circ$ ):

$$\begin{aligned} n_{\perp, \text{tilt}} &= [n_{\perp}^2 + \frac{1}{2}(n_{\parallel}^2 - n_{\perp}^2) \sin^2 \theta_{\text{tilt}}]^{1/2} \\ n_{\parallel, \text{tilt}} &= [n_{\perp}^2 + \frac{1}{2}(n_{\parallel}^2 - n_{\perp}^2) \cos^2 \theta_{\text{tilt}}]^{1/2}. \end{aligned} \quad (18)$$

The respective local field factors of the tilted configuration are assumed to be given in a similar form, i.e. they represent a combination of the local field factors  $f_{\perp}$  and  $f_{\parallel}$  determined previously for the nematic phase:

$$\begin{aligned} f_{\perp, \text{tilt}} &= f_{\perp} + \frac{1}{2}(f_{\parallel} - f_{\perp}) \sin^2 \theta_{\text{tilt}} \\ f_{\parallel, \text{tilt}} &= f_{\perp} + \frac{1}{2}(f_{\parallel} - f_{\perp}) \cos^2 \theta_{\text{tilt}}. \end{aligned} \quad (19)$$

Then the correction factor of a tilted nematic LC is given in analogy to equation (8) where the refractive indices and the local field factors of the tilted nematic phase are used instead of the respective values of the nematic LC. It becomes evident from equations (13), (18) and (19) that this factor depends on  $n_{\parallel}$  and  $n_{\perp}$  as well as on  $L_{\parallel}$  and  $L_{\perp}$  which itself represents functions of the molecular order parameter relative to the local nematic director,  $S_{\text{mol}}$ , given by equations (11) and (14).

The expression for the optical order parameter given in equation (5) in the case of an ensemble of molecules characterized by a local director tilted with respect to the optical axis should include additionally  $S_{\text{tilt}}$ , i.e.

$$S_{\text{opt}} = S_{\text{bond}} S_{\text{mol}} S_{\text{tilt}} \quad (20)$$

assuming that the distribution of the transition dipole moments around the molecular axis, the distribution of the molecular axes around the LC director, as well as the distribution of the local LC director around the pore axis, which is the optical axis of the system, are of rotational symmetry. This means that these three distributions should be independent of each other.  $S_{\text{tilt}}$  gives the order parameter of the tilt angle of the LC director with respect to the optical axis,  $\theta_{\text{tilt}}$ , analogously to equation (6).

With equation (20), the tilt order parameter of the local nematic director,  $S_{\text{tilt}}$ , can be obtained by a formula analogous to equation (16)

$$S_{\text{tilt}} = S_{\text{bond}}^{-1} S_{\text{mol}}^{-1} \frac{R - A(S_{\text{mol}}, \theta_{\text{tilt}})}{R + B(S_{\text{mol}}, \theta_{\text{tilt}})} \quad (21)$$

$A(S_{\text{mol}}, \theta_{\text{tilt}})$  and  $B(S_{\text{mol}}, \theta_{\text{tilt}})$  are expressions identical with those given in equation (17) where the correction factor,  $g(S_{\text{mol}})$ , and the refractive index of the horizontally polarized light,  $\bar{n}$ , are given by formulae analogous to equations (8) and (3), respectively. However in the present case the refractive indices  $n_{\perp, \text{tilt}}$  and  $n_{\parallel, \text{tilt}}$  should be used instead of  $n_{\perp}$  and  $n_{\parallel}$  and consequently, they represent functions of  $\theta_{\text{tilt}}$  in addition to  $S_{\text{mol}}$  as indicated by the arguments.

### 3.4. Anopore filled with liquid crystal

Anopore membranes consist of cubic  $\text{Al}_2\text{O}_3$  occupying a volume fraction of  $(1 - v) = 0.52$  [15] whereas the remaining fraction  $v = 0.48$ , the porosity, represents the pores and thus is taken up by the LC filled into it. The refractive index of the empty porous AP membrane material was determined previously in the spectral range of visible light [15]. Extrapolation of the data to the IR region gives a refractive index of  $n_{\text{AP}} = 1.604$  [15], a value slightly smaller than the refractive index  $n = 1.70$  of  $\text{Al}_2\text{O}_3$  at a wavelength of  $3 \mu\text{m}$  given in reference [27].

For symmetry reasons, AP-membranes should behave macroscopically as uniaxial crystals, the optical axis being aligned along the membrane normal. As long as the radius of the pores ( $R_{\text{pore}} = 0.1 \mu\text{m}$ ) is small with respect to the wavelength of light, the microscopically heterogeneous membrane can be regarded as a homogeneous medium whose ordinary and extraordinary indices of refraction are obtained by appropriate averaging. Applying classical theory of dielectric permittivity of ordered mixtures [28], the refractive indices of AP filled with nematic LC are

$$n_{\perp, \text{AP}} = \left[ n_{\text{AP}}^2 - \frac{2vn_{\text{AP}}^2(n_{\text{AP}}^2 - n_{\perp}^2)}{(1+v)n_{\text{AP}}^2 + (1-v)n_{\perp}^2} \right]^{1/2} \quad (22)$$

$$n_{\parallel, \text{AP}} = [n_{\text{AP}}^2 + v(n_{\parallel}^2 - n_{\text{AP}}^2)]^{1/2}$$

Note that in the present case the effective refractive indices deviate only insignificantly from the arithmetic mean of  $n_{\text{AP}}$  and  $n_{\perp}$  or  $n_{\parallel}$ , respectively. Consequently the birefringence of a nematic LC in AP is reduced at least by a factor of about 0.5 in comparison with the pure nematic phase. In the case of tilted nematic LC in AP, the effective refractive indices are calculated using equation (22) after substituting  $n_{\perp}$  and  $n_{\parallel}$  by  $n_{\perp, \text{tilt}}$  and  $n_{\parallel, \text{tilt}}$ , respectively.

## 4. Experimental results and discussion

### 4.1. 5CB in Anopore

#### 4.1.1. Spectral assignment and dichroism

Typical spectra of nematic 5CB in Anopore recorded at two perpendicular polarization directions are shown in figure 4. Five bands are selected as a first step for dichroism investigations: (i) the  $\text{C}\equiv\text{N}$  stretching vibration,  $\nu(\text{CN})$ , centred around  $2227 \text{ cm}^{-1}$ ; (ii, iii) two  $\text{CC}$ -benzene-skeletal in-plane deformations,  $\beta_{1500}(\text{CC})$  and  $\beta_{1600}(\text{CC})$ , centred around  $1495$  and  $1605 \text{ cm}^{-1}$ , respectively; (iv) the  $\text{CH}_2$  scissoring deformation,  $\delta(\text{CH}_2)$ , of the methylene groups around  $1467 \text{ cm}^{-1}$ ; and (v) the first overtone of the  $\text{CH}$ -out-of-plane deformation of the benzene  $\text{CH}$ -groups,  $\gamma_1(\text{CH})$ , around  $1930 \text{ cm}^{-1}$ .

The vibrations (i-iii) represent strong, well localized, characteristic group vibrations mostly free from overlapping bands. The transition moments point parallel to

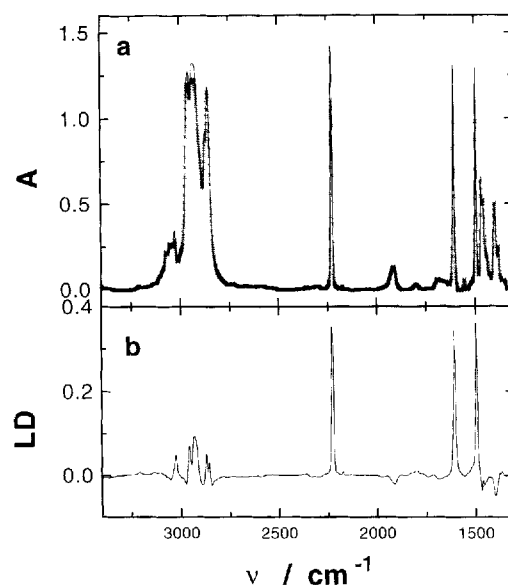


Figure 4. (a) Typical absorbance spectra of 5CB in Anopore recorded with the polarizer aligned vertically ( $A_{\perp}$ : -x-) and horizontally ( $A_{\parallel}$ : —). (b) Linear dichroism,  $LD = A_{\parallel} - A_{\perp}$ ; the temperature was  $25^{\circ}\text{C}$  and the angle of incidence  $\omega = 45^{\circ}$ .

the  $\text{C}\equiv\text{N}$  bond axis (i) and to the *para*-axis of the benzene rings (ii, iii), respectively. Commonly they are assumed to be directed parallel to the molecular long axis with  $\theta_{\text{bond}} = 0^{\circ}$  (cf. equation (4)) [17–19]. The transition moment of the  $\text{CH}_2$  scissoring deformation bisects the angle formed by the  $\text{H}-\text{C}-\text{H}$  bonds, and therefore on the average is expected to be perpendicular to the molecular long axis.

The  $\text{CH}$ -out-of-plane deformation was chosen by several authors because the corresponding transition moment is perpendicular to the benzene ring plane and consequently forms an angle  $\theta_{\text{bond}} \cong 90^{\circ}$  with the molecular long axis [18, 19, 29]. Unfortunately, the absorbance of the Anopore substrate shows a steep increase at wavenumbers smaller than  $1200 \text{ cm}^{-1}$  and therefore the  $\gamma(\text{CH})$  band around  $815 \text{ cm}^{-1}$  is located in a non-transparent spectral range of the sample. The first overtone of this vibration,  $\gamma_1(\text{CH})$ , however represents a well resolved, weak band around  $1930 \text{ cm}^{-1}$  suitable for quantitative analysis.

Upon varying the angle of incidence from  $0^{\circ}$  to  $60^{\circ}$ , the dichroic ratios corresponding to the transition dipoles parallel to the molecular long axis increase, whereas the dichroic ratios of the remaining two transitions,  $\delta(\text{CH}_2)$  and  $\gamma_1(\text{CH})$ , decrease (see figure 5). From this behaviour we conclude that the alignment of the 5CB molecules is predominantly parallel to the pore axes in agreement with the results of previous investigations on nematic liquid crystals confined within

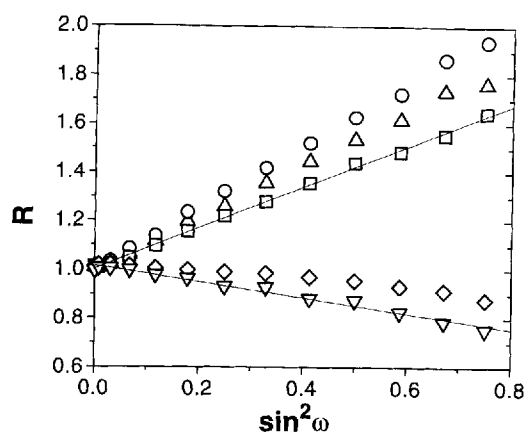


Figure 5. Dichroic ratios,  $R$ , of selected IR bands of 5CB in Anopore at 25°C as a function of  $\sin^2 \omega$  ( $\omega$  denotes the angle of incidence):  $\nu(\text{CN})$  ( $\square$ ),  $\beta_{1500}(\text{CC})$  ( $\triangle$ ),  $\beta_{1600}(\text{CC})$  ( $\circ$ ),  $\delta(\text{CH}_2)$  ( $\diamond$ ) and  $\gamma_1(\text{CH})$  ( $\nabla$ ). The lines represent linear fits with regression coefficients better than 0.9998.

micropores [2–4, 16]. Typically, the non-treated  $\text{Al}_2\text{O}_3$  walls of the membrane orient the nematic director along the axes of the cylindrical pores. The dichroic ratio data are well fitted by straight lines, thus indicating that the angular dependence is dominated by the  $\sin^2 \omega$  term explicitly given in equation (7). The additional  $\sin^2 \omega$  dependence implicit in the refractive index,  $\bar{n}$  (cf. equation (3)), obviously distorts the slopes only weakly. Using equation (3) and the mean refractive indices of nematic 5CB in AP, we estimate a difference  $\bar{n} - n_{\perp} < 0.02$  at the maximum angle of incidence  $\omega = 60^\circ$ . Consequently in the present case  $\bar{n} \approx n_{\perp}$  represents a good approximation which was used within the further calculations.

#### 4.1.2. Temperature dependence of the molecular order parameter

The temperature dependent dichroic ratios of the selected IR bands recorded at a fixed angle of incidence ( $\omega = 45^\circ$ ) reach a value  $R = 1$  at temperatures above the nematic–isotropic phase transition temperature of bulk 5CB,  $T_{\text{NI}} = 35\text{--}35.3^\circ\text{C}$  [30–32], thus indicating a loss of macroscopic orientational order of the 5CB molecules (see figure 6).

Deuterated 5CB- $d_2$  confined within polyvinylpyrrolidone treated polycarbonate Nucleopore membranes shows a temperature depression of  $T_{\text{NI}}$  between 1 and 2 K for pore radii of 0.03–0.5  $\mu\text{m}$  [2]. This effect was attributed mainly to impurities introduced by the Nucleopore filters. Identical N–I transition temperatures of bulk 5CB and of 5CB- $d_2$  confined within untreated Anopore membranes were reported by Crawford *et al.* [3] in accordance with our results. In Anopores, the authors found a reduction of the  $^2\text{H}$  NMR quadrupole

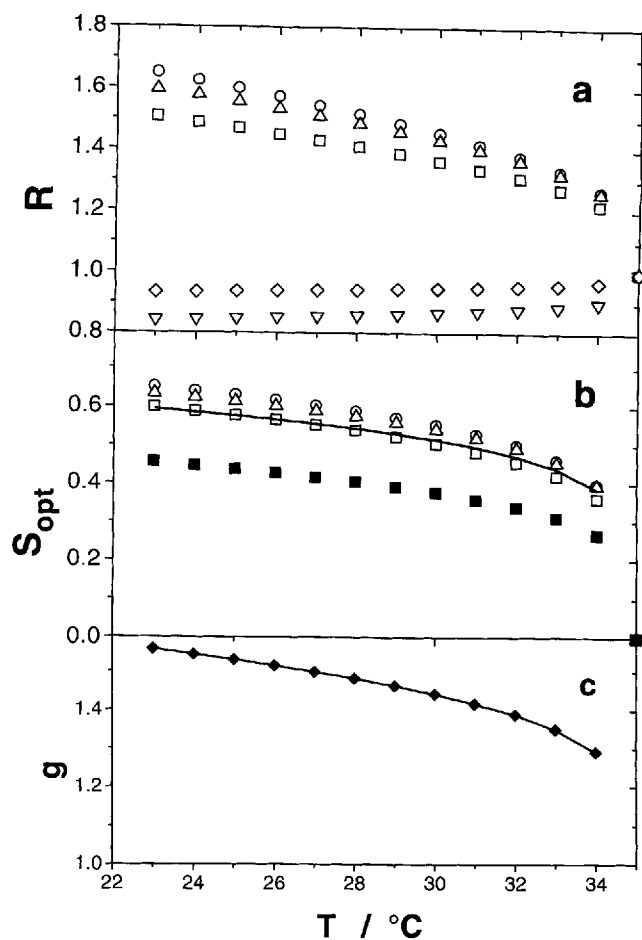


Figure 6. Temperature dependence of the dichroic ratio,  $R$  (a), of the optical order parameter,  $S_{\text{opt}}$  (b) and of the correction factor,  $g$  (c), of selected IR bands of 5CB in Anopore.  $R$  was recorded with an angle of incidence  $\omega = 45^\circ$ . Bands are denoted by the same symbols as in figure 5. In (b) the uncorrected order parameter of the CN-stretching band,  $S_{\text{opt}}^{(0)}(\text{CN})$ , and the corrected IR-order parameters of bulk 5CB taken from reference [19] are indicated by ( $\blacksquare$ ) and the continuous line (—), respectively.

splitting of 5CB- $d_2$  from about 20 kHz in the nematic phase down to about 200 Hz in the isotropic phase. The quadrupolar splitting frequency in the isotropic phase and its angular dependence identified the presence of surface-induced nematic order above the N–I phase transition temperature. This residual order was well explained by an alignment of the molecules within the first molecular layer induced by molecular interactions with the cavity wall. The fraction of 5CB molecules ordered at the wall of a cylindrical pore of radius  $R_{\text{pore}} = 0.1 \mu\text{m}$  can be estimated from the relation  $2l_0/R_{\text{pore}} \approx 4 \times 10^{-2}$ , assuming an interfacial thickness of the surface layer of  $l_0 = 2 \text{ nm}$  [3]. This means that the fraction of macroscopically oriented molecules decreases from nearly 1 in the nematic phase down to

about  $4 \times 10^{-2}$  in the isotropic phase, thus corresponding to the observed reduction of the quadrupolar splitting by about two orders of magnitude [3]. Analogously, we expect a decrease of the IR dichroic ratio in the isotropic phase,  $R_{\text{isotrop}}$ , to values corresponding to an ensemble averaged order parameter not exceeding  $\sim 10^{-2}$ . A rough estimation with a typical dichroic ratio below  $T_{\text{NI}}$  of  $R_{\text{nematic}} \approx 1.5$  yields  $|R_{\text{isotrop}} - 1| \approx |R_{\text{nematic}} - 1| \times 10^{-2} < 0.5 \times 10^{-2}$  (cf. equation (7)), a value hardly detectable assuming an experimental precision of  $R$  about  $\pm 2 \times 10^{-2}$ .

Consequently our investigation of the molecular order in microconfined structures will be restricted to temperatures below  $T_{\text{NI}}$ . In order to calculate the molecular order parameter,  $S_{\text{mol}}$ , of 5CB by means of equation (15), we assume that the validity of the empirical correlation between the refractive indices and  $S_{\text{mol}}$  established for bulk 5CB (cf. equation (11)) is preserved in the Anopore samples. Consequently the effective indices used are average values calculated from equations (22). A maximum Lorentz factor of  $L_{\perp, \text{max}} = 0.462$  was used in all calculations according to [19].

The molecular order parameter of 5CB was determined in an iterative way using the dichroic ratios,  $R(\text{CN})$ ,  $R(\text{CC}_{1600})$  and  $R(\text{CC}_{1500})$ , originating from the transition moments assumed to point along the long axis of 5CB. In these cases,  $S_{\text{mol}}$  coincides with  $S_{\text{opt}}$  because of  $\theta_{\text{bond}} = 0^\circ$  (i.e.  $S_{\text{bond}} = 1$ , cf. equation (5)). At first we calculate the uncorrected molecular order parameter,  $S_{\text{mol}}^{(0)}$ , from equation (16) with the correction factor  $g^{(0)} = 1$ . In the second step  $S_{\text{mol}}^{(0)}$  was inserted into equation (15) to yield a first approximation of the  $g$ -factor,  $g^{(1)} \neq 1$ , and, again using equation (16), a first corrected order parameter,  $S_{\text{mol}}^{(1)}$  was calculated. The sequence of  $S_{\text{mol}}^{(i)}$  values obtained with  $i = 0, 1, 2, \dots$ , by repeating this algorithm, converges rapidly. For  $i > 4$  the relative difference of the order parameter values in subsequent steps  $|(S_{\text{mol}}^{(i)} - S_{\text{mol}}^{(i-1)})/S_{\text{mol}}^{(i)}|$ , was less than  $3 \times 10^{-3}$ , and therefore  $S_{\text{mol}}^{(4)}$  was adopted as the resulting value of the molecular order parameter,  $S_{\text{mol}}$ .

Within the temperature range investigated the  $g$ -factor decreases gradually from 1.55 at 22°C to a value of 1.3 at 34°C (see figure 6(c)) thus leading to an order parameter,  $S_{\text{mol}}$ , increased by a factor of about 1.3 in comparison with the uncorrected value,  $S_{\text{mol}}^{(0)}$  (see figure 6(b)). The  $S_{\text{mol}}$  values calculated from  $R(\text{CN})$ ,  $R(\text{CC}_{1600})$  and  $R(\text{CC}_{1500})$  differ slightly, an effect reported previously also for bulk 5CB [18]. The ratios of the order parameters of the two skeletal deformations and the CN-stretching vibration,  $S_{\text{mol}}(\text{CC}_{1600})/S_{\text{mol}}(\text{CN})$  and  $S_{\text{mol}}(\text{CC}_{1500})/S_{\text{mol}}(\text{CN})$ , only weakly increase within the temperature range investigated by about 1–2% and adopt values of 1.06 and 1.08, respectively, at 25°C (data now shown). We arbitrarily select the CN order

parameter,  $S_{\text{mol}}(\text{CN})$  to characterize the average orientation of the 5CB molecules with respect to the nematic director.

The average orientation of a transition dipole with respect to the molecular axis is characterized by the 'bond' order parameter,  $S_{\text{bond}}$ , introduced in equation (5). It was calculated by means of equation (15) for the  $\delta(\text{CH}_2)$  and  $\gamma_1(\text{CH})$  bands, using the corresponding dichroic ratios and the  $S_{\text{mol}}(\text{CN})$  data. The bond order parameter of the  $\text{CH}_2$  scissoring vibration,  $S_{\text{bond}}(\text{CH}_2) \approx -0.06$ , represents an average over the flexible alkyl chain of the 5CB molecule and therefore its value is less negative than the order parameter,  $S_{\text{bond}}(\text{CH}) \approx -0.24$ , originating from the rigid biphenyl part. These  $S_{\text{bond}}$  data correspond to average bond angles of 57° and 65°, respectively. The last value agrees with the average bond angle of 63.6° calculated from the CH-out-of-plane vibration measured at 812  $\text{cm}^{-1}$  in bulk 5CB at 24.5°C [19].

The CN order parameters of 5CB in Anopore,  $S_{\text{mol}}(\text{CN})$ , adopt values very similar to that reported for bulk 5CB [17–19]. The authors however used different correction factors in order to compare their IR order parameters with NMR data published in reference [33]. The  $g$ -factors basing on the Lorentz field correction, originally introduced by Averyanov *et al.* [17] and used in [19] and by us, increase the uncorrected  $S_{\text{mol}}^{(0)}$  data significantly by a factor of about 1.3. The correction factor based upon the local field approximation of Vuks [34],  $g_{\text{Vuks}} = n_{\parallel}/n_{\perp}$ , was taken into account by Kiefer *et al.* [18]. In our investigation, the Vuks factor correction yields order parameters only about 1.03 times greater than the uncorrected data (data not shown). As discussed in reference [18], the degree of macroscopic alignment of bulk 5CB in the sample cell has an essential influence on the resulting molecular order parameters and possibly causes the discrepancies between the experimental results given in the literature. Regardless of these problems, we consequently applied the Lorentz field correction which apparently yields an upper limit of the molecular order parameter. Similarly the variation of the maximum value of the Lorentz factor,  $L_{\perp, \text{max}}$ , between 0.452 and 0.472 results in an increase of  $S_{\text{mol}}$  of about 10%.

#### 4.2. Lecithin treated Anopore

The temperature dependence of the dichroic ratio of the CN stretching band of 5CB in lecithin coated Anopore is depicted in figure 7. In contrast to the untreated Anopore, the dichroic ratios  $R(\text{CN})$ ,  $R(\text{CC}_{1600})$  and  $R(\text{CC}_{1500})$  corresponding to transition moments directed along the molecular axis of 5CB adopt values less than unity, whereas the dichroic ratios of the  $\delta(\text{CH}_2)$  and  $\gamma_1(\text{CH})$  bands originating from transition moments oriented perpendicular to the molecular axis

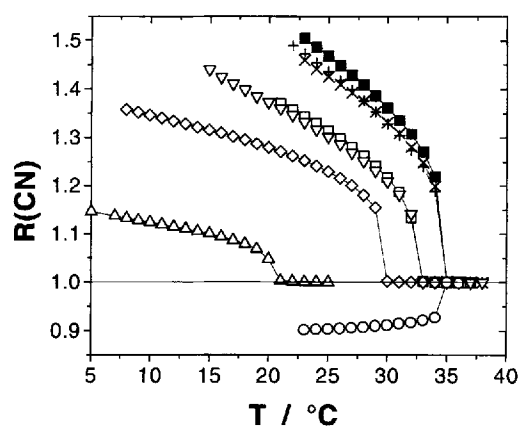


Figure 7. Temperature dependence of the dichroic ratio,  $R$ , of selected IR bands of 5CB in lecithin-coated Anopore ( $\circ$ ) and of 5CB/CB15 mixtures in Anopore. The mol fraction of CB15 was  $x = 0$  ( $\blacksquare$ ), 0.005 ( $+$ ), 0.014 ( $\times$ ), 0.02 ( $\square$ ), 0.05 ( $\nabla$ ), 0.1 ( $\diamond$ ), 0.25 ( $\triangle$ ).

are greater than unity (data not shown). These data indicate that the molecular long axis of 5CB on the average is tilted with respect to the pore axes by an angle greater than  $55^\circ$ , the magic angle, which corresponds to the dichroic ratio  $R = 1$  and thus to the optical order parameter  $S_{\text{opt}} = 0$ .

No significant shift of the nematic–isotropic transition temperature of 5CB was observed after lecithin coating. We therefore assume an identical temperature dependence of the molecular order parameter  $S_{\text{mol}}(\text{CN})$ , both in untreated and lecithin treated Anopore membranes. Note that  $S_{\text{mol}}$  is a measure of the mean orientation of the molecular long axes with respect to the uniaxial director in the untreated and to the tilted local director in the lecithin treated Anopore membranes. Using the  $S_{\text{mol}}(\text{CN})$  data for 5CB in untreated Anopore and the iterative algorithm presented in the previous section, we calculated  $S_{\text{tilt}}$  from equation (21) (see figure 8(b)). In view of the rough assumptions applied,  $S_{\text{tilt}}$  should be judged to be nearly constant within the temperature range investigated corresponding to a mean tilt angle of  $74$ – $78$  degrees. This nearly perpendicular arrangement of the local director with respect to the pore axes gives rise to values of the correction factor less than unity (data not shown). Ignoring the local field correction by using the  $S_{\text{mol}}$  data for untreated and lecithin treated AP obtained with the correction factor  $g = 1$ , yields a tilt order parameter  $S_{\text{tilt}}$ , slightly more negative than the corrected data (see figure 8(b)). This systematic shift of  $S_{\text{tilt}}$  corresponds to tilt angles of about  $78$ – $82$  degrees. Thus the local field correction is of only relatively weak influence (5%) on the tilt angles obtained.

In agreement with our findings, lecithin coated channels are known to induce a homeotropic orientation of

the director at the wall caused by the radial anchoring of the molecules [3, 4, 6]. These results demonstrate that a parallel as well as a perpendicular alignment of the nematic director with respect to the cylinder axes can be clearly distinguished by means of IR linear dichroism measurements on Anopore samples.

#### 4.3. 5CB/CB15 mixtures

CB15 represents a molecule similar to 5CB except for an asymmetrically attached methylene group in the  $\beta$ -position of the alkyl chain. In bulk samples, the addition of CB15 to nematic 5CB induces formation of a twisted nematic ordered liquid crystalline phase ( $N^*$ ). Its pitch decreases with increasing amount of CB15 added [14], accompanied by a decrease of the phase transition temperature between the  $N^*$  and isotropic phases,  $T_{\text{NI}}$ . A similar behaviour is observed after filling 5CB/CB15 mixtures into Anopore membranes. As indicated by a drop in the temperature dependence of the dichroic ratio, the  $T_{\text{NI}}$  values decrease down to  $20$ – $21^\circ\text{C}$  on increasing the weight fraction of CB15 within the mixture up to  $x_{\text{CB15}} = 0.25$  (cf. figure 7). No significant differences of the  $T_{\text{NI}}$  phase transition temperatures between bulk and AP samples were detected (data not shown). After scaling the abscissa to the reduced temperature,  $T_{\text{red}} = T/T_{\text{NI}}$ , it becomes evident that at constant  $T_{\text{red}}$ , the higher CB15 content induces a lower dichroic ratio and thus decreased CN optical order parameters. These remain positive however in all cases, in contrast to the 5CB filled lecithin coated Anopore (see figure 8(a)).

A tilted helicoidal director field of chiral LC phases inside the Anopore channels was suggested previously from optical [11] and NMR [12] investigations. Supposing that the molecular order parameter of the LC molecules with respect to the local director,  $S_{\text{mol}}$ , is identical with  $S_{\text{mol}}$  of pure 5CB in Anopore at the same reduced temperature, we determined the tilt order parameter,  $S_{\text{tilt}}$ , as described in the previous section (see figure 8(b)). Assuming a uniform tilt of the 5CB molecules, independent on their location within the Anopore channels, i.e.  $\theta_{\text{tilt}} = \text{const.}$ , the tilt angle of the local director with respect to the pore axis was calculated. Increase of the fraction of CB15 up to  $x_{\text{CB15}} = 0.25$  leads to an increase of  $\theta_{\text{tilt}}$  up to about  $40$  degrees (cf. figure 9(a), open symbols), accompanied by a decrease of the respective correction factors from about  $1.4$  for pure 5CB down to about  $1.1$  for  $x_{\text{CB15}} = 0.25$ .

As discussed previously [11, 12], an undisturbed helicoidal director field of twisted nematic LC phases inside the cylindrical pores is in contradiction to a parallel planar as well as a perpendicular orientation of the molecules at the walls. Therefore the model of a conic helical (CH) nematic director field for the adsorbed

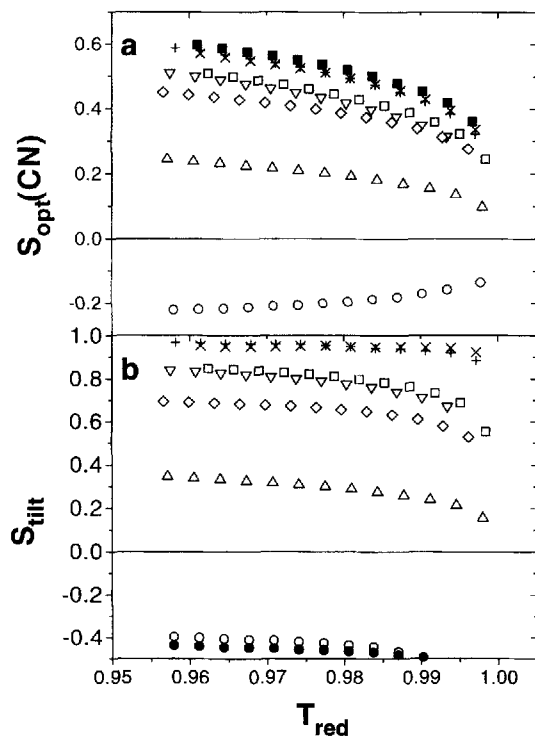


Figure 8. Temperature dependence of the optical order parameter,  $S_{opt}(CN)$  (a) and the tilt order parameter,  $S_{tilt}$  (b), of the CN-stretching bands of 5CB in lecithin-coated Anopore and of 5CB/CB15 mixtures in Anopore. The data are plotted against the reduced temperature,  $T_{red} = T/T_{NI}$ . The systems are labeled by the same symbols as in figure 7. The uncorrected tilt order parameter of 5CB in lecithin-coated Anopore is indicated by (●).

$N^*$  phase in untreated Anopore filters [11] assumes a nearly planar axial alignment of the molecules with  $\theta_{tilt} \approx 0^\circ$  at the surface. The tilt angle rises with increasing distance of the molecules from the wall and reaches the maximum value,  $\theta_{tilt}^{max}$ , after a distance characterized by  $\xi$ , the correlation length of the perturbation of the director field induced by the surface. The molecules are tilted radially, i.e. they are inclined normal to the surface and the tilt is assumed to screw along the cylinder axis similarly to the well known  $S^*$  structure.

Thus within the frame of this CH-model, the tilt angle is not a constant, but depends on the distance of a given molecule from the wall, at least for distances smaller than the respective correlation length. For  $\xi$  values covering only a few molecular layers, in Anopore the relation  $\xi \ll R_{pore}$  becomes valid and evidently the influence of the surface on the order parameter measured by means of the IR dichroic ratio can be neglected. On the other hand, for correlation lengths comparable with the cylinder radius, the IR-order parameter represents the mean value of the different local tilt angles of the LC molecules. We assume for a rough and simple estimation

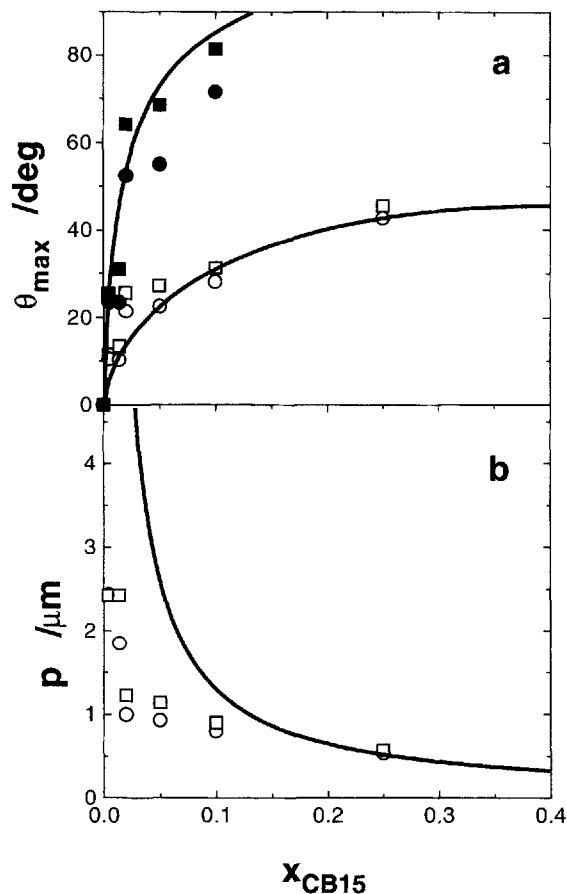


Figure 9. Maximum tilt angle,  $\theta_{max}$  (a) and pitch length,  $p$  (b), corresponding to the CH- and RTA-models, respectively, as a function of the weight fraction of CB15 added to 5CB,  $x_{CB15}$ .  $\theta_{max}$  and  $p$  were obtained from equations (26) and (27), respectively; at reduced temperatures  $T_{red} = 0.99$  (■, □) and 0.97 (●, ○). For the CH-model the  $\theta_{max}$ -data are shown for correlation lengths  $\xi \ll R_{pore}$  (open symbols) and  $\xi \approx R_{pore}$  (solid symbols). In (b) the dependence of the pitch length on the composition of bulk 5CB/CB15 mixtures taken from reference [14] is shown by the curve.

of a second limiting case with  $\xi \approx R_{pore}$  a linear relation between the local tilt angle,  $\theta_{tilt}$ , and  $r$  according to

$$\theta_{tilt}^{CH}(r) = \theta_{tilt}^{max} \frac{(R_{pore} - r)}{R_{pore}}. \quad (23)$$

$R_{pore} = 100$  nm denotes the cylinder radius and  $\theta_{tilt}^{max}$  is the maximum tilt angle reached in the pore centre.

In contrast to the CH-model, the radial twisted-axial (RTA) configuration assumes  $\theta_{tilt} = 0$  for  $r = 0$ , i.e. in the pore centre the molecules align along the cylinder axis. The tilt screws in the radial direction. Consequently, with increasing distance from the pore centre,  $r$ , the molecules are increasingly tilted tangentially, i.e. parallel to the surface, realizing in this way planar anchoring at

the wall. The tilt angle is given by

$$\theta_{\text{tilt}}^{\text{RTA}}(r) = \frac{2\pi}{p} r \quad (24)$$

where  $p$  denotes the pitch length of the radial helix.

The tilt order parameter measured on the IR experiment represents the ensemble average of the local order parameters within the Anopore cylinders, i.e.

$$S_{\text{tilt}} = \frac{2}{R_{\text{pore}}^2} \int_0^{R_{\text{pore}}} r^{\frac{1}{2}} [3 \cos^2 \theta_{\text{tilt}}(r) - 1] dr. \quad (25)$$

Inserting equations (23) and (24) into equation (25), one obtains after integration the mean tilt order parameters

$$S_{\text{tilt}}^{\text{CH}} = \frac{1}{4} \left( 1 + 3 \frac{\sin^2 \theta_{\text{tilt}}^{\text{max}}}{\theta_{\text{tilt}}^{\text{max}^2}} \right) \quad (26)$$

for the CH model and

$$S_{\text{tilt}}^{\text{RTA}} = \frac{1}{4} \left[ 1 - 3 \frac{\sin^2 \left( 2\pi \frac{R_{\text{pore}}}{p} \right)}{\left( 2\pi \frac{R_{\text{pore}}}{p} \right)^2} + 6 \frac{\cos \left( 2\pi \frac{R_{\text{pore}}}{p} \right) \sin \left( 2\pi \frac{R_{\text{pore}}}{p} \right)}{2\pi \frac{R_{\text{pore}}}{p}} \right] \quad (27)$$

for the RTA model.

Using the tilt order parameters obtained experimentally for different weight fractions of CB15, we determined the corresponding values of the maximum tilt angle,  $\theta_{\text{tilt}}^{\text{max}}$ , and pitch length,  $p$ , satisfying equations (26) and (27), respectively. For  $\xi \approx R_{\text{pore}}$  the maximum tilt angle in the pore centre reaches its limiting value of  $\theta_{\text{tilt}}^{\text{max}} = 90^\circ$  at about  $x_{\text{CB15}} \approx 0.15$ . The  $S_{\text{tilt}}$  data measured at  $x_{\text{CB15}} = 0.25$  yield maximum tilt angles  $\theta_{\text{tilt}}^{\text{max}} > 90^\circ$ , thus indicating in this case probably an overestimation of the correlation length  $\xi$ . Hence, within the frame of the model of conic helicoidal nematic director field (CH) our estimation gives the upper and lower limit of  $\theta_{\text{tilt}}^{\text{max}}$  corresponding to correlation lengths of  $\xi \approx R_{\text{pore}}$  and  $\xi \ll R_{\text{pore}}$ , respectively. The pitch lengths,  $p$ , of the radially twisted axial (RTA) configuration decrease with increasing fraction of the chiral dopant,  $x_{\text{CB15}}$ , (cf. figure 9(b)). In the corresponding bulk system, the pitch of the twisted nematic phase (N\*) is inversely proportional to the concentration of the dopant according to  $p = 0.13 \mu\text{m}/x_{\text{CB15}}$  for the 5CB/CB15 mixture at room temperature [14]. Our results indicate distinctly smaller values of  $p$  in the microconfined systems in comparison with the corresponding bulk phase for  $x_{\text{CB15}} < 0.2$ .

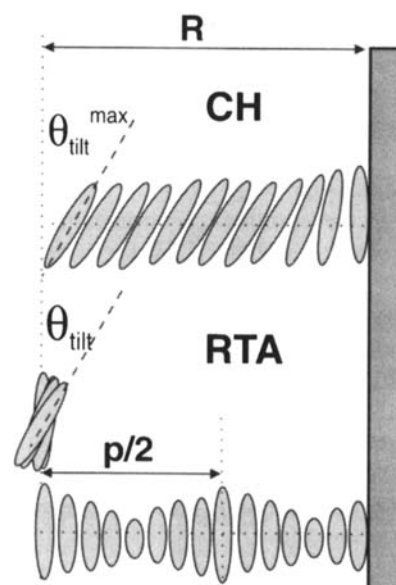


Figure 10. Schematic illustration of the conical helicoidal (top) and the radially twisted axial (bottom) configuration of the 5CB molecules in Anopore membranes.

An unambiguous model for the structure of the chiral confined director field is hardly to be established on the basis of the experimental facts available up to now. The tilt of the local director determined by means of the IR dichroic ratio and quantified in terms of the IR order parameter is not in contradiction to the CH or the RTA models (figure 10). However, a tilt angle of  $90^\circ$  as predicted by the axially twisted planar bipolar (ATPB) configuration is not confirmed by the results of the IR dichroism measurements.

## 5. Conclusions

The molecular order of LC molecules filled into cylindrically shaped pores of AP membranes was investigated by means of IR dichroism measurements. The arrangement of the molecules was characterized in terms of the order parameter of the molecular long axes calculated from the IR dichroic ratio. The experimental IR dichroic ratio data are corrected for local field effects within the frame of the ellipsoidal cavity model using the linear relation between the refractive indices and the molecular order parameter of bulk 5CB established empirically. The analysis of the data takes into account the refractive index of the  $\text{Al}_2\text{O}_3$  matrix of the AP membranes as well as the tilt of the LC molecules with respect to the cylinder axis.

In untreated AP membranes, 5CB forms a nematic phase with the molecular long axes oriented on average along the cylindrical pores. The nematic order is characterized by a similar temperature dependence of the

molecular order parameters in AP and bulk samples. Evidently the local order of the LC molecules is not influenced by the confining geometry of the Anopore matrix. Coating of the pore surface with amphiphilic lecithin gives rise to a perpendicular anchoring of the 5CB molecules. The perpendicular orientation of 5CB with respect to the pore walls is approximately preserved inside the pores, as indicated by the average tilt angle of about 80°. A twisted nematic bulk phase can be induced by adding CB15 to nematic 5CB. In AP, an increasing amount of the dopant CB15 causes an increase in tilt of the LC molecules relative to the axes of the pores. This behaviour can be interpreted in terms of a conical helicoidal (CH) or alternatively the radially twisted axial (RTA) arrangement of the LC molecules within the pores allowing no unequivocal decision between these models.

This work was supported by the Deutsche Forschungsgemeinschaft under grant SFB294. We would like to thank I. Friedemann who performed the birefringence measurements and B. Kohlstrunk for excellent technical assistance.

#### References

- [1] GOLEMME, A., ZUMER, S., ALLENDER, D. W., and DOANE, J. W., 1988, *Phys. Rev. Lett.*, **61**, 2937.
- [2] CRAWFORD, G. P., YANG, D. K., ZUMER, S., FINOTELLO, D., and DOANE, J. W., 1991, *Phys. Rev. Lett.*, **66**, 723.
- [3] CRAWFORD, G. P., STANNARIUS, R., and DOANE, J. W., 1991, *Phys. Rev. A*, **44**, 2558.
- [4] VRBANCIC, N., VILFAN, M., BLINC, R., DOLISEK, J., CRAWFORD, G. P., and DOANE, J. W., 1993, *J. chem. Phys.*, **98**, 3540.
- [5] FURNEAUX, R. C., RIGBY, W. R., and DAVIDSON, A. P., 1989, *Nature*, **337**, 147.
- [6] CRAWFORD, G. P., ONDRIS-CRAWFORD, J., ZUMER, S., and DOANE, J. W., 1993, *Phys. Rev. Lett.*, **70**, 1838.
- [7] ONDRIS-CRAWFORD, J., CRAWFORD, G. P., ZUMER, S., and DOANE, J., 1993, *Phys. Rev. Lett.*, **70**, 194.
- [8] LEQUEUX, F., and KLEMAN, M., 1988, *J. Phys. (Paris)*, **49**, 845.
- [9] CLADIS, P. E., WHITE, A. E., and BRINKMAN, W. F., 1979, *J. Phys. (Paris)*, **40**, 325.
- [10] BEZIC, J., and ZUMER, S., 1993, *Liq. Cryst.*, **14**, 1695.
- [11] SCHMIEDEL, H., STANNARIUS, R., FELLER, G., and CRAMER, C., 1994, *Liq. Cryst.*, **17**, 323.
- [12] SCHMIEDEL, H., STANNARIUS, R., CRAMER, C., FELLER, G., and MÜLLER, H.-E., 1995, *Mol. Cryst. liq. Cryst.*, **262**, 167.
- [13] KRALJ, S., and ZUMER, S., 1993, *Liq. Cryst.*, **15**, 521.
- [14] ONDRIS-CRAWFORD, R. J., AMBROZIC, M., DOANE, J. W., and ZUMER, S., 1994, *Phys. Rev. E*, **50**, 4773.
- [15] CRAMER, C., BINDER, H., and SCHMIEDEL, H., *Mol. Cryst. liq. Cryst.* (accepted for publication).
- [16] CRAWFORD, G. P., STEELE, L. M., ONDRIS-CRAWFORD, R., INNACCHIONE, G. S., YEAGER, C. J., and DOANE, J. W., 1992, *J. chem. Phys.*, **96**, 7788.
- [17] AVERYANOV, E. M., SHUIKOV, V. A., SHABANOV, V. F., and ADOMENAS, P. V., 1982, *Kristallografija*, **27**, 333.
- [18] KIEFER, R., and BAUR, G., 1989, *Mol. Cryst. liq. Cryst.*, **174**, 101.
- [19] WU, S.-T., 1987, *Appl. Opt.*, **26**, 3434.
- [20] SAUPE, A., and MAIER, W., 1961, *Z. Naturforsch.*, **16a**, 816.
- [21] BLINOV, L. M., KIZEL, V. G., RUMYANTSEV, V. G., and TITOV, V. V., 1975, *Sov. Phys. Crystallogr.*, **20**, 750.
- [22] HOLMGREN, A., JOHANSSON, B. A., and LINDBLOM, G., 1987, *J. phys. Chem.*, **91**, 5298.
- [23] DUNMUR, D. A., 1971, *Chem. Phys. Lett.*, **10**, 49.
- [24] AVERYANOV, E. M., and SHABANOV, V. F., 1978, *Kristallografija*, **23**, 320.
- [25] AKUTSU, H., KYOGOKU, Y., NAKAHARA, H., and FUKUDA, K., 1975, *Chem. Phys. Lip.*, **15**, 222.
- [26] AVERYANOV, E. M., DENITE, J., KOREZ, A. J., SOROKIN, A. V., and SHABANOV, V. F., 1980, *Kristallografija*, **25**, 319.
- [27] SCHROEDER, H., and NEUROTH, N., 1967, *Optik*, **26**, 381.
- [28] WIENER, O., 1912, *Abh. Sächs. Ges. Wiss. Math. Phys.*, **32**, 5298.
- [29] UMEMURA, J., 1988, *Surface*, **26**, 180.
- [30] Merck Ltd product information.
- [31] BREDEL, P. A., and MULKENS, Z. C. H., 1987, *Mol. Cryst. liq. Cryst.*, **147**, 107.
- [32] GRAY, G. W., HARISON, K. J., and NASH, J. A., 1975, *Pramana Suppl.*, **1**, 381.
- [33] EMSLEY, J. W., LUCKHURST, G. R., and STOCKLEY, C. P., 1981, *Mol. Phys.*, **44**, 565.
- [34] VUKS, M. F., 1966, *Optika i Spektroskopija*, **20**, 361.